Performance Analysis of Pre-Equalized Multilevel Partial Response Schemes

M. Guenach*, L. Jacobs+, B. Kozicki*, and M. Moeneclaey+
*Alcatel-Lucent Bell Labs, +Ghent University, Belgium

Abstract—In order to achieve high speed on electrical interconnects, channel attenuation at high frequencies must be dealt with by proper transceiver design. In this paper we investigate finite-complexity MMSE pre-equalization under an average transmit power constraint, to compensate for channel distortion in the case of both full-response and precoded partial response signaling with L-PAM mapping, and consider the resulting error performance for symbol-by-symbol detection and sequence detection. For a representative electrical interconnect, we point out that the constellation size (2-PAM or 4-PAM), the type of signaling (full response or partial response), the detection method (symbol-by-symbol detection or sequence detection) and the number of pre-equalizer taps should be carefully selected in order to achieve satisfactory error performance at high data rates. For several scenarios, precoded duobinary 4-PAM is found to yield the best error performance for given average transmit power.

I. INTRODUCTION

All types of telecommunications equipment rely on a form of electrical interconnects e.g. chip-to-chip, chip-to-module. Over the last decade the requirements for electrical interconnect speed have evolved from hundreds of Mbit/s to multiple tens of Gbit/s [1]. Regardless of the advancements in channel design, signals experience degradation during transmission due to channel imperfections e.g. conductive and dielectric losses, impedance discontinuities, noise coupling, cross-talk and mode conversion [2].

Collectively, these impairments result in inter-symbol interference (ISI) and increased noise in the received signal which reduces signal integrity and directly affects the achievable error rate of the link. The modulation and equalization are the main design parameters in this small-scale context. At the modulation level, a vast majority of standard electrical interconnect systems operate with non-return to zero (NRZ) or pulse amplitude modulation with 4 levels (4-PAM) [3]. Despite its simplicity, NRZ modulation requires a large amount of equalization for high-speed electrical interconnect which motivates the use of partial response duobinary modulation as proposed in [4]. By design, in partial response signaling [5] a controlled intersymbol-interference amount is introduced to spectrally shape the signal, such that the signal power is more concentrated at the lower frequencies. Low-complexity signal detection in the case of partial response involves a modulo operation at the receiver; alternatively, at the expense of higher complexity, maximum likelihood sequence detection exploiting the inherent redundancy in the signal [7] can be exploited.

Several authors have investigated pre-equalization in the context of high-speed electrical interconnects. The authors of [11] consider duobinary signaling, and use a frequency-domain fitting to determine the coefficients of a finite impulse response (FIR) linear pre-equalizer. In [12], the combination of a programmable 2-tap pre-equalizer at the transmitter and an adaptive 4-tap decision-feedback equalizer (DFE) at the receiver are investigated for NRZ signaling. In [4], a 2-tap pre-equalizer with fractional delay is optimized numerically to minimize a semi-analytically computed bit error rate (BER). In [10], the coefficients of a 6-tap equalizer are represented by 4 bits, and their values are optimized by means of a numerical search to mimimize data-dependent jitter. In [9], a combination of an FIR pre-equalizer and a one-tap DFE is considered for partial response signaling; a minimum mean-square error (MMSE) criterion is used to determine the filter taps. Most of these papers consider the eye opening (simulated or measured) or the measured BER as a performance measure.

In the present contribution we focus on linear MMSE pre-equalization with limited complexity, for generic multi-level mapping and full-response or precoded partial-response signaling. Section II considers the optimization of not only the filter tap values at the transmitter but also the scaling factor applied to the signal at the input of the detector; we point out that this approach yields a smaller mean-square error (MSE) compared to the case where (as in [9]) only the filter taps are optimized. Unlike other contributions on pre-equalization, the analytical derivation of the optimum filter taps and scaling factor is performed by transforming the MSE into an equivalent but simpler expression that allows a geometrical interpretation. The error performance of the detector is investigated in section III. Accurate upper and lower bounds on the symbol error probability, that take into account the presence of noise and residual ISI, are presented in the case of symbol-by-symbol detection; these bound are computationally less complex than the semi-analytically computed error rate from [4].

II. PRE-EQUALIZATION OF PARTIAL-RESPONSE SYSTEMS

We consider the precoded partial response (PR) system from Fig. 1, characterized by a polynomial $h_{\mathcal{T}}(D) = 1 + \sum_{m>0} h_{\mathcal{T},m} D^m$ with integer coefficients. At the transmitter, the precoder converts a sequence of i.i.d. L-ary digits $\{a_n\}$, that are uniformly distributed over the set $\{0, 1, ..., L-1\}$, into a sequence $\{b_n\}$, according to $b_n = \left[a_n - \sum_{m>0} h_{\mathcal{T},m} b_{n-m}\right]_L$ where $[x]_L$ denotes the modulo-L reduction of x to the half-open interval $[0, L)$. We restrict our attention to the case where L is an integer power of 2. The resulting precoder output $\{b_n\}$ consists of i.i.d. L-ary digits

that are uniformly distributed over the set $\{0, 1, ..., L-1\}$. The sequence $\{b_n\}$ is mapped to the symbol sequence $\{d_n\}$ according to $d_n = 2b_n - L + 1$, so that d_n belongs to the L-PAM constellation $\mathcal{A}_d = \{-(L-1), -(L-3), ..., L-3, L-1\}$; we denote $\sigma_d^2 = \mathbb{E}[d_n^2] = \frac{L^2-1}{3}$. The L-PAM symbols $\{d_n\}$ are applied to a linear pre-equalizer that operates at the symbol rate $1/T$, where T stands for the symbol interval. Denoting the pre-equalizer coefficients by $\{g_m\}$, the corresponding pre-equalizer transfer function is $G(e^{j2\pi fT}) = \sum_m g_m e^{-j2\pi fmT}$. The output of the pre-equalizer is fed to a *fixed* unit-energy transmit filter $H_{\text{tr}}(f)$. Introducing the notation $< X(e^{j2\pi fT}) > = T \int_{-1/(2T)}^{1/(2T)} X(e^{j2\pi fT}) df$, the resulting transmit symbol energy E_{tr} is obtained as

$$E_{\text{tr}} = \sigma_d^2 \langle |G(e^{j2\pi fT})|^2 R_{\text{tr}}(e^{j2\pi fT}) \rangle = \sigma_d^2 \mathbf{g}^T \mathbf{R}_{\text{tr}} \mathbf{g} \quad (1)$$

where $\mathbf{g}$ is a vector containing the pre-equalizer coefficients, $\mathbf{R}_{\text{tr}}$ is a Toeplitz matrix determined by $(\mathbf{R}_{\text{tr}})_{m,n} = \int |H_{\text{tr}}(f)|^2 e^{j2\pi f(m-n)T} df$ and $R_{\text{tr}}(e^{j2\pi fT}) = \frac{1}{T} \sum_n |H_{tr}(f - \frac{n}{T})|^2$. When $H_{\text{tr}}(f)$ is a unit-energy square-root Nyquist filter, $\mathbf{R}_{\text{tr}}$ becomes the identity matrix, and $R_{\text{tr}}(e^{j2\pi fT}) = 1$. The transmitted signal enters a channel with transfer function $H_{\text{ch}}(f)$, and is affected by additive white Gaussian noise (AWGN) with spectral density $N_0/2$. The received signal is applied to *fixed* filter $H_{\text{rec}}(f)$. The receiver filter output is sampled at the symbol rate at instants $nT + \tau$, and the resulting samples are multiplied by a scaling factor $1/\xi$. Introducing $H_c(f) = H_{\text{tr}}(f) H_{\text{ch}}(f) H_{\text{rec}}(f)$, the scaled sample z_n can be represented as

$$z_n = (1/\xi) \cdot \sum_m d_{n-m} (\sum_k g_k h_{m-k}) + \nu_n \quad (2)$$

where $h_m = h_c(mT + \tau)$ is the sample of the impulse response $h_c(t)$ of $H_c(f)$, taken at $mT + \tau$, and $\sigma_\nu^2 = \sigma^2/\xi^2$ with $\sigma^2 = (N_0/2) \int |H_{\text{rec}}(f)|^2 df$ denoting the noise variance at the output of the receiver filter. The sampling delay τ is a design parameter, which affects the value of the coefficients $\{h_m\}$. We intend to select the coefficients $\{g_m\}$ and the scaling factor $1/\xi$ such that z_n in (2) is close to w_n given by

$$w_n = d_n + \sum_{m>0} h_{\mathcal{T},m} d_{n-m} \quad (3)$$

subject to the transmit power constraint (1). Note from (3) that we take for w_n a specific linear combination of the current and past symbols $\{d_m\}$, where $\{h_{\mathcal{T},m}\}$ denote the integer coefficients of the partial response polynomial $h_{\mathcal{T}}(D)$ that has been used in the precoding operation ; it is explained in section III how the receiver detects the symbol a_n from a noisy version of w_n. The special case where $h_{\mathcal{T}}(D) = 1$ is referred to as full response (FR) signaling; in the case of FR, the precoding and (3) reduce to $b_n = a_n$ and $w_n = d_n$, respectively.
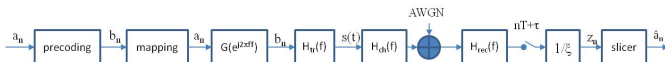
Figure 1. Precoded partial response system

For the sake of practical implementation, we focus on a pre-equalizer with a finite number (L_g) of coefficients, i.e.,

$\mathbf{g} = (g_0, g_1, ..., g_{L_g-1})^T$; at the end of this section we point out that restricting our attention to a causal pre-equalizer represents no loss of generality. Introducing the matrix $\mathbf{H}$ and the vector $\mathbf{h}_{\mathcal{T}}$, with $(\mathbf{H})_{m,n} = h_{m-n}$ and $(\mathbf{h}_{\mathcal{T}})_m = h_{\mathcal{T},m}$, we rewrite (2) as

$$z_n = w_n + \sum_m d_{n-m} (\frac{1}{\xi} \mathbf{H} \mathbf{g} - \mathbf{h}_{\mathcal{T}})_m + \nu_n \quad (4)$$

where the second term in (4) denotes residual ISI. Assuming that the impulse response $h_c(t)$ has a finite duration, the coefficients h_m are zero for $m \notin \{-L_{h,\min}, -L_{h,\min} + 1, ..., L_{h,\max}\}$, so that (at most) $L_h = L_{h,\min} + L_{h,\max} + 1$ coefficients are nonzero; note that L_h depends on the duration of $h_c(t)$, while $L_{h,\min}$ is a function of the sampling delay τ. Hence, $\mathbf{H}$ and $\mathbf{h}_{\mathcal{T}}$ have nonzero rows only for the row index ranging from $-L_{h,\min}$ to $L_{h,\max}+L_g-1$ and from 0 to $L_{\mathcal{T}}-1$, respectively. Therefore, the summation index m in (4) can be restricted to the finite range $M_{\text{fin}} = (-L_{h,\min}, -L_{h,\min} + 1, ..., L_{h,\max} + L_g - 1) \cup (0, 1, ..., L_{\mathcal{T}} - 1)$. The closeness of z_n to w_n is expressed by the mean-square error (MSE) $\mathbb{E}[(z_n - w_n)^2]$, given by

$$\mathbb{E}[(e_n)^2] \triangleq \mathbb{E}[(z_n - w_n)^2] = \sigma_d^2 ||\frac{1}{\xi} \mathbf{H} \mathbf{g} - \mathbf{h}_{\mathcal{T}}||^2 + \frac{\sigma^2}{\xi^2} \quad (5)$$

In the following, we will select the pre-equalizer coefficients $\mathbf{g}$ and the scaling factor ξ such that (5) is minimized under the constraint (1).

Before minimizing the MSE, we will turn (5) into an equivalent expression, which allows a geometrical interpretation. Considering the singular-value decomposition (SVD) $\mathbf{H}\mathbf{R}_{\text{tr}}^{-0.5} = \mathbf{U}\mathbf{\Sigma}\mathbf{V}^T$, where $\mathbf{R}_{\text{tr}}^{-0.5}$ is the inverse of $\mathbf{R}_{\text{tr}}^{0.5}$, with $\mathbf{R}_{\text{tr}}^{0.5}\mathbf{R}_{\text{tr}}^{0.5} = \mathbf{R}_{\text{tr}}$, we define the invertible transforms $\mathbf{g} = \mathbf{R}_{\text{tr}}^{-0.5}\mathbf{V}\mathbf{x}$ and $\mathbf{h}_{\mathcal{T}} = \mathbf{U}\mathbf{q}$, which convert the MSE (5) into

$$\mathbb{E}[(e_n)^2] = \sigma_d^2 \sum_{m \in M_1} (\frac{1}{\xi} s_m x_m - q_m)^2 + \sigma_d^2 \sum_{m \in M_0} q_m^2 + \frac{\sigma^2}{\xi^2} \quad (6)$$

and the constraint (1) into $\sigma_d^2 \sum_{m \in M_{\text{fin}}} x_m^2 = E_{\text{tr}}$ where $M_0 \subset M_{\text{fin}}$ is the subset of indices for which the corresponding eigenvalues of $\mathbf{H}\mathbf{R}_{\text{tr}}^{-1}\mathbf{H}^T$ are zero, $M_1 = M_{\text{fin}} \setminus M_0$, and $s_m = (\mathbf{\Sigma})_{m,m}$ for $m \in M_1$. Denoting the m-th column of $\mathbf{U}$ by $\mathbf{U}^{<m>}$, the first term in (6) depends on the projection $\sum_{m \in M_1} q_m \mathbf{U}^{<m>}$ of $\mathbf{h}_{\mathcal{T}}$ on the column space of $\mathbf{H}$, and is a function of both $\mathbf{x}$ and ξ; this term can be cancelled by a proper selection of the pre-equalizer taps. The second term in (6) is not affected by $\mathbf{x}$ nor ξ, and therefore represents the irreducible part of the MSE; this term equals σ_d^2 times the squared magnitude of the component of $\mathbf{h}_{\mathcal{T}}$ that is orthoghonal to the column space of $\mathbf{H}$. The sum of both these terms denotes the contribution from the residual ISI, and equals the first term of (5). The third term in (6) represents the noise contribution, which is affected by the scaling factor ξ. Minimization of the MSE (6) will yield optimum values of $(\mathbf{x}, \xi)$; having obtained $\mathbf{x}$, the actual optimum pre-equalizer coefficients $\mathbf{g}$ are computed as $\mathbf{g} = \mathbf{R}_{\text{tr}}^{-0.5}\mathbf{V}\mathbf{x}$.

A suboptimum approach, adopted in [9], consists of minimizing the MSE for a fixed ξ, and then selecting ξ such that the constraint imposed by the transmitter is satisfied. When

using for the MSE the expression (6) rather than (5), this yields $x_m = \xi_{\text{sub}} q_m / s_m$ for $m \in M_1$ (which cancels the first term in (6)) and $x_m = 0$ for $m \in M_0$, with $\xi_{\text{sub}}^2 \sigma_d^2 \sum_{m \in M_1} \frac{q_m^2}{s_m^2} = E_{\text{tr}}$. The corresponding MSE is given by

$$(\mathbb{E}[(e_n)^2])_{\text{sub}} = \sigma_d^2 \sum_{m \in M_0} q_m^2 + \mu \sigma_d^2 \sum_{m \in M_1} \frac{q_m^2}{s_m^2} \qquad (7)$$

where $\mu = \sigma^2 / E_{\text{tr}}$. Essentially, this solution minimizes the residual ISI under the transmit energy constraint. This approach is not optimum, because during the optimization over $\mathbf{x}$ the coupling between $\mathbf{x}$ and ξ, introduced by the energy constraint , is ignored. The approach that is optimum in terms of MSE involves the *joint* minimization of (6) w.r.t. $\mathbf{x}$ and ξ under the energy constraint. The resulting minimum MSE (MMSE) solution is $x_m = \xi_{\text{mmse}} q_m s_m / (s_m^2 + \mu)$ for $m \in M_1$ and $x_m = 0$ for $m \in M_0$, with $\xi_{\text{mmse}}^2 \sigma_d^2 \sum_{m \in M_1} \frac{q_m^2 s_m^2}{(s_m^2 + \mu)^2} = E_{\text{tr}}$. The resulting minimum MSE is given by

$$(\mathbb{E}[(e_n)^2])_{\text{mmse}}$$
$$= \mu^2 \sigma_d^2 \sum_{m \in M_1} \frac{q_m^2}{(s_m^2 + \mu)^2} + \sigma_d^2 \sum_{m \in M_0} q_m^2$$
$$+ \mu \sigma_d^2 \sum_{m \in M_1} \frac{q_m^2 s_m^2}{(s_m^2 + \mu)^2} \qquad (8)$$
$$= \mu \sigma_d^2 \sum_{m \in M_1} \frac{q_m^2}{s_m^2 + \mu} + \sigma_d^2 \sum_{m \in M_0} q_m^2 \qquad (9)$$

The sum of the first and second term in (8) denotes the contribution from the residual ISI, which is larger than the corresponding contribution (first term in (7)) for the suboptimum pre-equalizer; however, as $\xi_{\text{mmse}}^2 > \xi_{\text{sub}}^2$, the MMSE pre-equalizer gives rise to a smaller noise contribution (third term in (8) smaller than second term in (7)). The net effect is a smaller total MSE for the MMSE solution (first term in (9) smaller than first term in (7)). At high SNR (i.e., $\mu \ll \min_{m \in M_1} s_m^2$), both approaches yield essentially the same MSE.

The MSE performance of the pre-equalizer depends on the sampling delay τ at the receiver. This delay can be decomposed as $\tau = n_s T + \epsilon T$, where $n_s = \lfloor \tau / T \rfloor$ and $0 \leq \epsilon < 1$; $n_s T$ and ϵT denote the integer delay and fractional delay, respectively. Basically, $n_s T$ and ϵT should be selected such that the sampling delay compensates for the delay introduced by the transfer function $H_c(f)$ from the transmit filter input to the receive filter output. When the implementation of the sampling clock does not allow modifying the fractional delay ϵT, only $n_s T$ can be adjusted, by simply introducing the appropriate integer delay at the sampler. Having considered a causal pre-equalizer $\mathbf{g} = (g_0, g_1, ..., g_{L_g - 1})^T$ is without loss of generality: a non-causal FIR pre-equalizer can be turned into a causal pre-equalizer that yields the same performance, by introducing additional delay at the transmitter and applying the same additional delay to the sampler.

III. ERROR PERFORMANCE ANALYSIS

We consider a detector that ignores the presence of the residual ISI in (4), and therefore assumes $z_n = w_n + \nu_n$,

with w_n given by (3). It can be verified that

$$[w_n]_{2L} = [2a_n - (L-1) \, h_{\mathcal{T}}(D)|_{D=1}]_{2L} \qquad (10)$$

so that the modulo-$2L$ reduction of w_n depends only on the digit a_n. Based on the relation (10), symbol-by-symbol detection can be performed on $[z_n]_{2L}$. The corresponding decision $\hat{a}_n$ is given by $\hat{a}_n = \alpha$, where $\alpha \in \{0, 1, ..., L-1\}$ minimizes $F([z_n]_{2L}, [w(\alpha)]_{2L})$, with $w(\alpha) = 2\alpha - (L-1) \, h_{\mathcal{T}}(D)|_{D=1}$ and $F(x,y) = \min(|x-y|, 2L - |x-y|)$. The resulting symbol error probability $P_E = \Pr[\hat{a}_n \neq a_n]$ in the absence of residual ISI is well approximated by $P_E = 2Q(\frac{1}{\sigma_\nu})$ [8], where $Q(x)$ is the complement of the cumulative distribution function of a zero-mean Gaussian random variable with unit variance. A better error performance is achieved by applying sequence detection, i.e., we look for the sequence $\{\hat{a}_n\}$ for which the corresponding sequence $\{\hat{w}_n\}$ minimizes the squared Euclidean distance $\sum_n (z_n - \hat{w}_n)^2$; sequence detection exploits the correlation that is present in $\{w_n\}$ due to PR signaling, and is implemented efficiently by means of the Viterbi algorithm. In the absence of residual ISI, the resulting P_E is essentially proportional to $Q(\frac{d_{min}}{2\sigma_\nu})$, where $d_{\min}^2$ denotes the minimum of the squared Euclidean distances between allowed sequences $\{w_n\}$ [8]; hence, for given $h_{\mathcal{T}}(D)$, sequence detection yields a performance gain (expressed in dB) of $10 \log(\frac{d_{min}^2}{4})$ over symbol-by-symbol detection. In the case of FR, we have $w_n = 2a_n - (L-1)$, so that symbol-by-symbol detection gives rise to $\hat{a}_n = \alpha$, where $\alpha \in \{0, 1, ..., L-1\}$ minimizes $|z_n - w(\alpha)|$; in the absence of residual ISI, this yields $P_E = 2\frac{L-1}{L} Q(\frac{1}{\sigma_\nu})$. The actual error performance of the detectors described above is deteriorated by the presence of residual ISI. Here we investigate the performance of the symbol-by-symbol detector, taking into account the residual ISI that results from a finite-length pre-equalizer. The performance of the Viterbi-based sequence detection will be assessed by means of computer simulations in section IV.

Taking into account that the symbol-by-symbol detection of the digit a_n in the case of PR signaling is based on $[z_n]_{2L}$, a correct symbol decision is obtained when $z_n - w_n \in \mathbb{S}$, with $\mathbb{S} = \bigcup_{i \in \mathbb{Z}} (2iL - 1, 2iL + 1)$. The sample z_n from (4) can be represented as $z_n = w_n + \text{ISI}_n + \nu_n$, where

$$\text{ISI}_n = \sum_m d_{n-m} e_m \qquad (11)$$

represents the residual ISI. The coefficients e_m in (11) are obtained as $e_m = h_{\text{tot},m} - h_{\mathcal{T},m}$, where $\{h_{\text{tot},m}\}$ are the coefficients of the filter $H_{\text{tot}}(e^{j2\pi fT})$ from the pre-equalizer input to the scaled output of the receive filter, i.e., $H_{\text{tot}}(e^{j2\pi fT}) = \frac{1}{\xi} G(e^{j2\pi fT}) \cdot H(e^{j2\pi fT})$ with $H(e^{j2\pi fT}) = \sum_m h_m e^{-j2\pi fmT}$; note that $H_{\text{tot}}(e^{j2\pi fT})$ does not depend on the PAM constellation size. Let us denote by $\mathbf{d}_n$ the vector of data symbols that contribute to ISI_n; in order to emphasize the dependence of ISI_n on $\mathbf{d}_n$, we write $\text{ISI}_n = \text{isi}(\mathbf{d}_n)$. The symbol error probability, defined as $P_E = \Pr[\hat{a}_n \neq a_n]$, can be expressed as $P_E = \mathbb{E}[P_E(\mathbf{d}_n)]$, where the expectation is over the symbol vector $\mathbf{d}_n$, and $P_E(\mathbf{d}_n) = \Pr[\text{isi}(\mathbf{d}_n) + \nu_n \notin \mathbb{S}]$

is the symbol error probability conditioned on $\mathbf{d}_n$. One can easily verify that

$$P_{\mathrm{E}}(\mathbf{d}_n) = 1 - \sum_{i \in \mathbb{Z}} Q(\frac{\Delta_{i,-}(\mathbf{d}_n)}{\sigma_\nu}) - Q(\frac{\Delta_{i,+}(i,\mathbf{d}_n)}{\sigma_\nu}) \quad (12)$$

where $\Delta_{i,-}(\mathbf{d}_n) = 2iL - 1 - \mathrm{isi}(\mathbf{d}_n)$ and $\Delta_{i,+}(\mathbf{d}_n) = 2iL + 1 - \mathrm{isi}(\mathbf{d}_n)$. The infinite summation over i in (12) can be truncated to only a few terms; more specifically, when for given $\mathbf{d}_n$ we have $\mathrm{isi}(\mathbf{d}_n) \in [(2i_0 - 1)L, (2i_0 + 1)L]$, the summation index can be safely restricted to $i \in \{i_0 - 1, i_0, i_0 + 1\}$.

Let us restrict our attention to the practically important case where the pre-equalizer has been designed such that no decision errors occur when noise is absent, i.e., the eye opening at the receive filter output is not closed at the decision instants $nT + \tau$. Denoting by $\mathrm{isi}_{\max}$ the maximum of $|\mathrm{isi}(\mathbf{d}_n)|$ over all possible $\mathbf{d}_n$, the eye is open when $\mathrm{isi}_{\max} < 1$ (implying that $|\mathrm{isi}(\mathbf{d}_n)| < 1$ for all $\mathbf{d}_n$). It follows from (11) that

$$\mathrm{isi}_{\max} = (L - 1) \sum_m |e_m| \quad (13)$$

Assuming that $\mathrm{isi}_{\max} < 1$ and $\sigma_\nu^2 \ll 1$, the conditional error probability $P_{\mathrm{E}}(\mathbf{d}_n)$ is well approximated by keeping in (12) only the terms with $i = 0$, i.e.,

$$P_{\mathrm{E}}(\mathbf{d}_n) = Q(\frac{1 + \mathrm{isi}(\mathbf{d}_n)}{\sigma_\nu}) + Q(\frac{1 - \mathrm{isi}(\mathbf{d}_n)}{\sigma_\nu}) \quad (14)$$

Using the approximation (14) instead of the exact expression (12), we obtain

$$P_{\mathrm{E}} = 2\mathbb{E}\left[Q(\frac{1 + \mathrm{isi}(\mathbf{d}_n)}{\sigma_\nu})\right] \quad (15)$$

where we have taken into account that the vectors $\mathbf{d}_n$ and $-\mathbf{d}_n$ have the same probability. In the absence of residual ISI, (15) reduces to $P_{\mathrm{E}} = 2Q\left(\frac{1}{\sigma_\nu}\right)$.

Let us denote by M_{e} the set of indices m for which e_m in (11) is nonzero, and by N_{e} the number of elements in M_{e}. The exact computation of the expectation $\mathbb{E}[P_{\mathrm{E}}(\mathbf{d}_n)]$ then involves a summation of $L^{N_{\mathrm{e}}}$ terms, which becomes computationally prohibitive for large N_{e}. This problem can be circumvented by computing bounds on P_{E} in the following way. First, we partition M_{e} into the subsets M_{large} and M_{small} where M_{large} contains the indices m of the N_1 coefficients e_m with the largest magnitudes, and M_{small} contains the indices of the $N_2 = N_{\mathrm{e}} - N_1$ remaining coefficients e_m with the smaller magnitudes; we have $0 \leq N_1 \leq N_{\mathrm{e}}$. Next, we decompose ISI_n as $\mathrm{ISI}_n = \mathrm{ISI}_{1,n} + \mathrm{ISI}_{2,n}$, where $\mathrm{ISI}_{1,n} = \sum_{m \in M_{\mathrm{large}}} d_{n-m}e_m$ and $\mathrm{ISI}_{2,n} = \sum_{m \in M_{\mathrm{small}}} d_{n-m}e_m$. Denoting $\mathbf{d}_{1,n} = \{d_{n-m}, m \in M_{\mathrm{large}}\}$ and $\mathbf{d}_{2,n} = \{d_{n-m}, m \in M_{\mathrm{small}}\}$, we write $\mathrm{ISI}_{1,n} = \mathrm{isi}_1(\mathbf{d}_{1,n})$ and $\mathrm{ISI}_{2,n} = \mathrm{isi}_2(\mathbf{d}_{2,n})$. Taking into account that $Q(u + v) + Q(u - v)$ is an increasing function of $|v|$ when $u > 0$ and assuming $\mathrm{isi}_{\max} < 1$, the error probability (15) can be bounded as $P_{\mathrm{E,low}} \leq P_{\mathrm{E}} \leq P_{\mathrm{E,up}}$, where

$$P_{\mathrm{E,low}} = 2\mathbb{E}\left[Q(\frac{1 + \mathrm{isi}_1(\mathbf{d}_{1,n})}{\sigma_\nu})\right] \quad (16)$$

$$P_{\mathrm{E,up}} = \mathbb{E}\left[Q(\frac{\Delta_{\mathrm{up},+}}{\sigma_\nu}) + Q(\frac{\Delta_{\mathrm{up},-}}{\sigma_\nu})\right] \quad (17)$$

In (17), we have $\Delta_{\mathrm{up},+} = 1 + \mathrm{isi}_1(\mathbf{d}_{1,n}) + \mathrm{isi}_{2,\max}$ and $\Delta_{\mathrm{up},-} = 1 + \mathrm{isi}_1(\mathbf{d}_{1,n}) - \mathrm{isi}_{2,\max}$, with $\mathrm{isi}_{2,\max} = (L - 1) \sum_{m \in M_{\mathrm{small}}} |e_m|$ denoting the maximum of $|\mathrm{isi}_2(\mathbf{d}_{2,n})|$ over $\mathbf{d}_{2,n}$. As compared to (15), which involves a summation over $L^{N_{\mathrm{e}}}$ terms, the expectations in (16) and (17) over $\mathbf{d}_{1,n}$ represent summations over only L^{N_1} terms; the selection of N_1 is a trade-off between high accuracy (large N_1) and low computational complexity (small N_1). A looser upper bound on (15) is obtained as $P_{\mathrm{E}} \leq 2Q\left(\frac{1 - \mathrm{isi}_{\max}}{\sigma_\nu}\right)$ where $\mathrm{isi}_{\max}$ is given by (13), with the summation index restricted to $m \in M_{\mathrm{e}}$. This upper bound is obtained from (15) by assuming that $\mathrm{isi}(\mathbf{d}_n) = -\mathrm{isi}_{\max}$ for all $\mathbf{d}_n$, and relates the error performance to the noise variance σ_ν^2 and the eye opening $1 - \mathrm{isi}_{\max}$ at the input of the detector.

In the case of FR signaling, the detection does not involve the modulo operation. In order to obtain the symbol error probability for given L and $\{e_m\}$ for FR signaling, we first consider the error probability $P_{\mathrm{E}}(\alpha) = \Pr[\hat{d}_n \neq d_n \,|\, d_n = \alpha]$ conditioned on the transmitted symbol, and next we average $P_{\mathrm{E}}(\alpha)$ over $\alpha \in \mathcal{A}_d$. The resulting error probability is obtained as $P_{\mathrm{E}} = P_{\mathrm{E,in}} + P_{\mathrm{E,out}}$, with

$$P_{\mathrm{E,in}} = \frac{2}{L} \sum_{\alpha \in \mathcal{A}_{d,\mathrm{in}}} \mathbb{E}\left[Q(\frac{1 + e_0\alpha + \mathrm{isi}_0(\mathbf{d}_n^{(0)})}{\sigma_\nu})\right] \quad (18)$$

$$P_{\mathrm{E,out}} = \frac{2}{L} \mathbb{E}\left[Q(\frac{1 + (L - 1)e_0 + \mathrm{isi}_0(\mathbf{d}_n^{(0)})}{\sigma_\nu})\right] \quad (19)$$

where $\mathcal{A}_{d,\mathrm{in}} = \{-(L-3), -(L-5), ..., (L-3)\}$ is the set of inner constellation points, $\mathbf{d}_n^{(0)}$ collects the data symbols that contribute to ISI_n from (11) with the exception of the useful symbol d_n,

$$\mathrm{isi}_0(\mathbf{d}_n^{(0)}) = \sum_{m \neq 0} d_{n-m}e_m \quad (20)$$

denotes the ISI caused by the symbols contained in $\mathbf{d}_n^{(0)}$, and the expectation in (18-19) is with respect to $\mathbf{d}_n^{(0)}$. In the absence of residual ISI, FR gives rise to $P_{\mathrm{E}} = 2\frac{L-1}{L}Q\left(\frac{1}{\sigma_\nu}\right)$. Using a similar reasoning as for PR signaling, upper and lower bounds on P_{E} are easily derived when $\mathrm{isi}_{\max} < 1$, by bounding the individual terms in (18-19).

IV. NUMERICAL RESULTS

In this section, we will derive numerical performance results, based on a channel transfer function obtained from simulation of an electrical backplane interconnect including two traces on daughter boards, two high-speed backplane connectors and a 10-cm long differential trace on a printed circuit board. The pre-equalizer performance results have been optimized not only over the pre-equalizer coefficients $\{g_n\}$ and the scaling factor $1/\xi$, but also over the sampling delay τ (which we restrict to be a multiple of $T/10$). Besides FR signaling, we will consider PR signaling with polynomials $h_{\mathcal{T}}(D) = 1 + D$ and $h_{\mathcal{T}}(D) = (1 + D)^2 = 1 + 2D + D^2$, which will be referred to as duobinary (DB) and double duobinary (DDB), respectively.
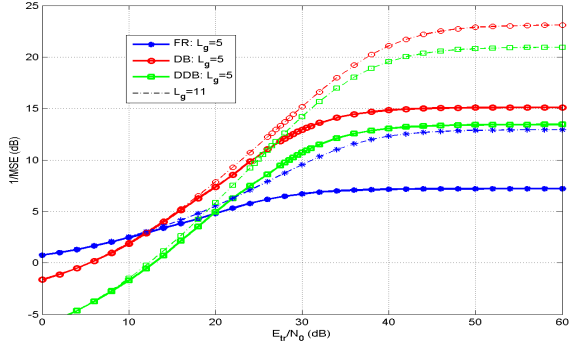
Figure 2. $1/\text{MSE}$ as a function of E_{tr}/N_0 for 2-PAM at 100 Gbaud.
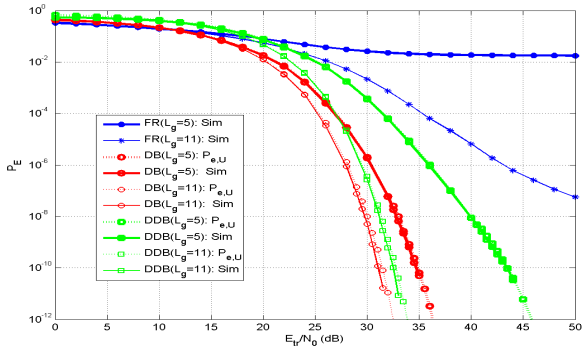
Figure 3. P_{E} as a function of E_{tr}/N_0 for symbol-by-symbol detection (2-PAM, 100 Gbaud)) .

For FR, DB and DDB signaling, Fig. 2 shows $1/\text{MSE}$ as a function of E_{tr}/N_0 in the case of 2-PAM, with MSE denoting the mean square error (9) after scaling the receiver filter output sample. Note that for these systems the transmit power is given by $P_{\text{tr}} = E_{\text{tr}}/T$, with $1/T = 100$ Gbaud. For increasing E_{tr}/N_0, MSE converges to the last summation in (9), which is caused by $\mathbf{h}_{\mathcal{T}}$ not belonging to the column space of $\mathbf{H}$; this gives rise to the $1/\text{MSE}$ floor occurring at large E_{tr}/N_0 in Fig. 2. For moderate and large E_{tr}/N_0, $1/\text{MSE}$ considerably increases when going from 5 to 11 pre-equalizer taps: the residual ISI is substantially reduced when using more pre-equalizer taps, yielding a much larger $1/\text{MSE}$ floor. We observe that PR signaling significantly reduces MSE as compared to FR, with DB slightly outperforming DDB. Taking into account that for 2-PAM and 4-PAM we have $\sigma_{\text{d}}^2 = 1$ and $\sigma_{\text{d}}^2 = 5$, respectively, it follows from (9) that the curves of $1/\text{MSE}$ versus E_{tr}/N_0 for 4-PAM at 100 Gbaud (i.e., 4-PAM operating at 200 Gbit/s) are obtained by shifting downward by 7 dB the curves from Fig. 2.

We consider the symbol error probability P_{E} resulting from symbol-by-symbol detection, assuming MMSE pre-equalization with 5 taps and 11 taps, for FR, DB and DDB signaling; the constellation is 2-PAM. Fig. 3 shows as a function of E_{tr}/N_0 the simulated error probability, along with the upper bound (17) on P_{E} for the cases where $\text{isi}_{\max}$ from (13) does not exceed 1; when computing (17) we have selected N_1 such that the horizontal shift between the upper

bound and the lower bound (16) at high E_{tr}/N_0 is less than about 0.5 dB, so that the upper bound can be considered as sufficiently tight. For FR signaling with 5-tap and 11-tap pre-equalization, we get $\text{isi}_{\max} > 1$, which results in a symbol error probability floor because of eye closure. We observe that FR is significantly outperformed by both DB and DDB at moderate to high E_{tr}/N_0, and that DB performs better than DDB; this behavior is in agreement with the $1/\text{MSE}$ curves from Fig. 2.
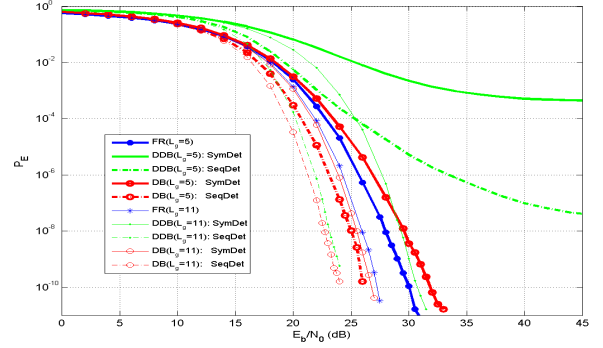
Figure 4. P_{E} as a function of E_{b}/N_0 for 4-PAM operating at 50 Gbaud with 5 and 11-tap pre-equalizer.

Whereas for symbol-by-symbol detection DB performs better than DDB, we see that DDB outperforms DB when sequence detection is applied (figure not included). The benefit from sequence detection is larger for DDB than for DB, because the former yields the larger minimum squared Euclidean distance $d_{\min}^2$ between allowed sequences $\{w_n\}$: for DB and DDB we have $d_{\min}^2 = 8$ and $d_{\min}^2 = 16$, respectively.

Here we investigate the error performance for 4-PAM operating at half the baudrate and half the bandwidth (50 Gbaud and 25 GHz, respectively) as compared to the 100 Gbit/s 2-PAM transmission; hence, the channel is less dispersive in the case of 4-PAM. As in this second scenario the 2-PAM and 4-PAM transmissions operate at the same bitrate, it is convenient to compare their error performance for given E_{b}/N_0, with $E_{\text{b}} = E_{\text{tr}}/\log_2(L)$ representing the transmitted energy per bit (for 2-PAM, we have $E_{\text{b}}/N_0 = E_{\text{tr}}/N_0$); note that $P_{\text{tr}} = E_{\text{b}}R_b$, with $R_b = \log_2(L)/T$ denoting the bitrate.

Fig. 4 shows the 50 Gbaud 4-PAM error performance related to the second scenario, for $L_g = 5$ and $L_g = 11$, respectively. For $L_g = 5$, DDB with symbol-by-symbol detection and with sequence detection both exhibit an error floor, caused by the large ISI peak power. We observe that for $L_g = 5$ with symbol-by-symbol detection, FR outperforms DB (2 dB difference at low P_{E}), whereas DB yields the better performance when sequence detection is used (3-4 dB better than FR at low P_{E}). The residual ISI is substantially reduced when taking $L_g = 11$, so that error floors are absent. For $L_g = 11$ with symbol-by-symbol detection, DB is slighly better than FR (1.5 dB difference at low P_{E}), which in turn outperforms DDB; error performance is further improved by means of sequence detection, with DB slightly outperforming DDB (less than 0.5 dB difference at low P_{E}).

	2-PAM, 100 Gbit/s	4-PAM, 100 Gbit/s	4-PAM, 200 Gbit/s
	5/11 taps	5/11 taps	11 taps
FR	- - -/—	5.7/3.3 dB	- - -
DB SymDet	10.5/7.0 dB	7.3/2.8 dB	19.1 dB
DDB SymDet	18.4/8.5 dB	- - -/6.6 dB	- - -
DB SeqDet	5.7/3.9 dB	2.4/0.0 dB	13.7 dB
DDB SeqDet	4.8/1.8 dB	- - -/0.1 dB	14.7 dB

Table I

RELATIVE TRANSMIT POWER $P_{\mathrm{tr}}/P_{\mathrm{ref}}$ AT A TARGET P_{E} OF 10^{-9}

Let us define the power efficiency as the average transmit power P_{tr} needed to achieve $P_{\mathrm{E}} = 10^{-9}$; the smaller P_{tr}, the more efficient the considered scheme. Using $P_{\mathrm{tr}} = E_{\mathrm{b}}R_{\mathrm{b}} = E_{\mathrm{tr}}/T$, the power efficiency of a particular scheme can be derived from the corresponding curve showing P_{E} versus E_{b}/N_0 or E_{tr}/N_0 when N_0 is known. Noting by P_{ref} the power efficiency for precoded DB 4-PAM with sequence detection at 100 Gbit/s and 11-taps pre-equalizer, Table I shows the relative power efficiency $P_{\mathrm{tr}}/P_{\mathrm{ref}}$ (expressed in dB) for the different modulation schemes; the entry "- - -" indicates the occurrence of an error probability floor, which either exceeds 10^{-9} or yields an unacceptably large transmit power to reach $P_{\mathrm{E}} = 10^{-9}$. Fig. 4 shows that, for precoded DB 4-PAM with sequence detection at 100 Gbit/s and 11-taps pre-equalizer, $P_{\mathrm{E}} = 10^{-9}$ is achieved at $E_{\mathrm{b}}/N_0 = 23.4$ dB, yielding $(P_{\mathrm{ref}})_{\mathrm{dBm}} = 23.4 + 110 + (N_0)_{\mathrm{dBm/Hz}}$; for instance, when N_0 = -140 dBm/Hz, we have P_{ref} = -6.6 dBm.

Let us first focus on 2-PAM operating at 100 Gbit/s. Considering a 5-taps pre-equalizer and using symbol-by-symbol detection, DB yields the best performance ($P_{\mathrm{tr}}/P_{\mathrm{ref}}$ = 10.5 dB) among the modulations considered; using sequence detection, DDB is to be preferred ($P_{\mathrm{tr}}/P_{\mathrm{ref}}$ = 4.8 dB), yielding an improvement of 5.7 dB over symbol-by-symbol detection. Increasing the number of pre-equalizer taps to 11, the best modulation when using symbol-by-symbol detection is DB ($P_{\mathrm{tr}}/P_{\mathrm{ref}}$ = 7.0 dB), whereas sequence detection improves the power efficiency by 5.2 dB, i.e., for DDB ($P_{\mathrm{tr}}/P_{\mathrm{ref}}$ = 1.8 dB). Hence, moving from 5 taps to 11 taps and from symbol-by-symbol detection to sequence detection yields performance gains on the order of 3 dB and 5 dB, respectively.

In the case of 4-PAM operating at 100 Gbit/s, the best schemes for 5-taps pre-equalization with symbol-by-symbol detection and sequence detection are FR ($P_{\mathrm{tr}}/P_{\mathrm{ref}}$ = 5.7 dB) and DB ($P_{\mathrm{tr}}/P_{\mathrm{ref}}$ = 2.4 dB), respectively, with the latter providing a 3.3 dB gain over the former. When using 11 taps, DB is the best modulation for both symbol-by-symbol detection ($P_{\mathrm{tr}}/P_{\mathrm{ref}}$ = 2.8 dB) and sequence detection ($P_{\mathrm{tr}}/P_{\mathrm{ref}}$ = 0.0 dB), with the latter performing 2.8 dB better than the former. Note that at 100 Gbit/s, for a given number of taps and a given detection method, the best schemes for 4-PAM outperform the best schemes for 2-PAM, by roughly 4.5 dB and 2 dB for symbol-by-symbol detection and sequence detection, respectively.

Finally, we consider 4-PAM operating at 200 Gbit/s, using 11-tap pre-equalization. Table I shows that DB is the best scheme, for both symbol-by-symbol detection ($P_{\mathrm{tr}}/P_{\mathrm{ref}}$ = 19.1 dB) and sequence detection ($P_{\mathrm{tr}}/P_{\mathrm{ref}}$ = 13.7 dB), with the latter offering a 5.4 dB performance advantage. Compared to the best schemes for 100 Gbit/s with 5 taps (11 taps) pre-equalization, doubling the bitrate from 100 Gbit/s to 200 Gbit/s gives rise to a power penalty of 13.4 dB (16.3 dB) for symbol detection and 11.3 dB (13.7 dB) for sequence detection.

V. CONCLUSIONS

In this contribution, we have investigated limited-complexity pre-equalization for full response and partial response signaling in the context of high-rate data transmission on electrical interconnects. We have presented the mathematical framework for deriving the MMSE pre-equalizer coefficients under an average transmit power contraint. For a specific representative interconnect, we have determined the symbol error performance for various combinations of data rate (100 Gbit/s, 200 Gbit/s), type of signaling (FR, DB, DDB), constellation size (2-PAM, 4-PAM), detection method (symbol-by-symbol detection, sequence detection) and pre-equalizer complexity (5 taps, 11 taps). The various schemes have been compared in terms of the required transmit power in order to achieve a symbol error probability of 10^{-9}.

This study illustrates the need for carefully selecting the constellation size, the signaling format, the detection method and the pre-equalizer complexity in order to achieve a satisfactory error performance for transmission at 100 Gbit/s and beyond on electrical interconnects.

REFERENCES

[1] D. Law, D. Dove, J. D'Ambrosia, M. Hajduczenia, M. Laubach, S. Carlson, "Evolution of ethernet standards in the IEEE 802.3 working group," IEEE Communications Magazine, vol. 51, no. 8, pp.88-96, August 2013.

[2] Jun Fan; Xiaoning Ye; Jingook Kim; Archambeault, B.; Orlandi, A.; , , "Signal Integrity Design for High-Speed Digital Circuits: Progress and Directions," IEEE Transactions on Electromagnetic Compatibility, vol.52, no.2, pp.392-400, May 2010.

[3] D. Law, D. Dove, J. D'Ambrosia, M. Hajduczenia, M. Laubach and S. Carlson, "Evolution of ethernet standards in the IEEE 802.3 working group", IEEE Communications Magazine, vol. 51, no. 8, pp. 88-96, August 2013.

[4] J. H. Sinsky, M. Duelk and A. Adamiecki, "High-speed electrical backplane transmission using duobinary signaling", IEEE Transactions on Microwave Theory and Techniques, vol. 53, no. 1, pp. 152-160, January 2005.

[5] A. Lender, "The duobinary technique for high-speed data transmission", American Institute of Electrical Engineers, Part I: Communication and Electronics, Transactions of the , vol. 82, no. 2, pp. 214-218, May 1963.

[6] R. D. Gitlin, J. F. Hayes and S. B. Weinstein, 'Data communication principles', Plenum Press, New York and London, 1992.

[7] H Kobayashi , "Correlative Level Coding and Maximum Likelihood Decoding", IEEE Transaction on Information Theory, vol. 17, no. 5, pp. 586 - 594, September 1971.

[8] J. G. Proakis, 'Digital Communications', McGraw-Hill, 2000.

[9] M. R. Ahmadi, J. Moon and R. Harjani, "Constrained Partial Response Receivers for High-Speed Links", IEEE Transactions on Circuits and Systems II: Express Briefs, vol. 55, no. 10, pp. 1006-1010, October 2008.

[10] M. Bichan and A. C. Carusone, "A 6.5 Gb/s Backplane Transmitter with 6-tap FIR Equalizer and Variable Tap Spacing", IEEE 2008 CICC, pp. 611 – 614, 21-24 Sept. 2008.

[11] D. Chen, B. Wang, B. Liang, D. Cheng and T. Kwasniewski, "Design and Optimization of Edge Equalizer for High-Speed Electrical Backplane", 7th International Conference on Information, Communications and Signal Processing (ICICS 2009), pp. 1-5, 8-10 Dec. 2009.

[12] V. Balan, et al., "A 4.8–6.4-Gb/s Serial Link for Backplane Applications Using Decision Feedback Equalization", IEEE Journal Solid-State Circuits, Vol. 40, No. 9, pp. 1957-1967, September 2005